



CrossMark
 click for updates

Cite this: *RSC Adv.*, 2017, 7, 2676

Ultraviolet upconversion emission of Pb²⁺ ions sensitized by Yb³⁺-trimers in CaF₂

Tuerxun Aidilibike,^{ab} Junjie Guo,^a Lili Wang,^a Xiaohui Liu,^a Yangyang Li^a and Weiping Qin^{*a}

Under 978 nm near infrared (NIR) excitation, ultraviolet (UV) upconversion (UC) emissions from Pb²⁺ ions in CaF₂:Pb²⁺,Yb³⁺ were first observed at room temperature. The UC emission centered at ~383 nm was ascribed to the ³P₀ → ¹A_{1g} (¹S₀) transition of Pb²⁺ ions. From transient measurements, the UC process was found to be dominated by the energy transfer process: three excited Yb³⁺ ions simultaneously transfer their energy to one Pb²⁺ ion. With the increase in Pb²⁺ concentration, the cooperative luminescence from 3-Yb³⁺ clusters decreased gradually until it was extinguished. The cooperative sensitization to one Pb²⁺ ion comes from three excited Yb³⁺ ions, which is a four-ion process and exhibits a third power dependence on the NIR pumping power.

Received 17th October 2016
 Accepted 9th December 2016

DOI: 10.1039/c6ra25344j

www.rsc.org/advances

Optical frequency UC is a luminescence technology developed since the 1960s. Thanks to the successful fabrications of powerful infrared (IR) diode lasers and heavy metal fluoride glasses, visible (VIS) upconversion luminescence (UCL) including red, green, and blue has been performed since the 1980s.^{1–7} With the development of manufacturing technology for nanometer materials, UCL labelling has gathered great attention.^{8–11} The study on UCL was derived from the detection of IR light; however, it has a great number of potential applications in the fields of solid-state lasers, 3D displays, IR quantum counters, optical probes in fluorescent imaging techniques, anti-counterfeiting, NIR photocatalysis, and temperature sensors.^{6,7,9,10,12–15} Most of UC materials are rare-earth doped solid compounds; in which, a lanthanide ion absorbs more than one photon with lower energy and converts them to one photon with higher energy by using its metastable energy levels. Yb³⁺ ion has been extensively adopted as a sensitizer in UC processes because it has a long excited state lifetime and a relatively large absorption cross-section in the NIR region.¹⁶

No UCL from Pb²⁺ ions have been observed until now, although the down-conversion (DC) luminescence of Pb²⁺ ions in the UV and VIS regions has been reported and applied.^{17–19} As we know, the absorption and emission bands of Pb²⁺ ions usually appear in the UV region, and their electronic configuration is 6s² in the ground state (the ¹S₀ level) and (6s¹)(6p¹) in the excited states. The ¹S₀ ground state is expressed by ¹A_{1g} and

has an even parity. The excited state expressed by (6s¹)(6p¹) has an odd parity and consists of triplet states (³P₀, ³P₁, and ³P₂) and singlet excited state ¹P₁. After absorbing a UV photon (~330 nm), Pb²⁺ ion make an optical transition from ³P₀ to ¹A_{1g}.^{18,20} The energy difference between the ground state and the triplet state of Pb²⁺ is higher than the energy of two 980 nm photons or two excited Yb³⁺ ions. Such an energy-level characteristic determines that neither the energy of two 978 nm photons nor the energy of an excited Yb³⁺-dimer (two excited Yb³⁺ ions) can excite or sensitize a Pb²⁺ ion efficiently. Although, in the view of energy, three-photon excitation indeed can lead to the UV UCL of Pb²⁺ with a very low probability,¹⁶ however, until now, there has been no report on the UCL of Pb²⁺ ions under NIR excitation. Even so, the cooperative energy transfer from three or four excited Yb³⁺ ions (Yb³⁺-trimer or Yb³⁺-tetramer) can excite Pb²⁺ ion from the view of energy.

Cooperative transition usually means the physical processes in which identical ions or atoms simultaneously make transitions by absorbing (or emitting) one photon with the sum of all transition energies, or transferring their energies to another ion or atom. Cooperative transition includes cooperative luminescence (CL), cooperative absorption (CA), and cooperative energy transfer (CET) and is closely relative to clustered lanthanide ions in solid hosts. Clusters made of lanthanide ions can easily form in many materials, especially in alkaline-earth fluoride crystal AF₂ (A = Ca, Sr, Ba). When a lanthanide ion with +3 oxidation state is doped in an alkaline-earth fluoride, non-equilibrium of charge arises in the lattice due to the lanthanide ion usually occupy the position of an alkaline-earth ion with +2 oxidation state. The non-equilibrium of charge produces crystal defects such as the interstitials of F⁻ ions and cation vacancies in order to compensate excess plus charges, which gives non-uniform distribution of lanthanide ions.

^aState Key Laboratory on Integrated Optoelectronics, College of Electronic Science and Engineering, Jilin University, Changchun, Jilin 130012, China. E-mail: wpqin@jlu.edu.cn

^bYili Normal University, Electronic and Information Engineering, Laboratory on Micro-Nano Electro Biosensor and Bionic Devices, Yining, Xinjiang 835000, China



Different clusters, such as dimers, trimers, and even hexamers, can form in crystal lattices depending on the kind of lanthanide ions and their doping densities.^{21,22} The first observations of cooperative absorption and cooperative luminescence of Yb³⁺ dimers were reported in 1961 and 1970,^{23,24} respectively. Since then, cooperative transitions of Yb³⁺-dimers have been investigated in many Yb³⁺-doped materials.^{25–27} Recently, Qin *et al.* reported the triplet cooperative luminescence (TCL) at ~343 nm from three excited Yb³⁺ ions (Yb³⁺-trimer) and the cooperative energy transfer from four excited Yb³⁺ ions (Yb³⁺-tetramer) to one Gd³⁺ ion, which open the way to investigate the cooperative transitions of many-body systems.^{28,29} Furthermore, by considering the electric multipole interactions between ions and using the coupled wave functions of a many-lanthanide-ion system, Qin *et al.* proposed main cooperative transition mechanisms in a multi-ion system and calculated their probabilities.³⁰

In the present work, we report the first experimental observation of UV UCL peaked at 383 nm from Pb²⁺ ions sensitized by three excited Yb³⁺ ions cooperatively.

The XRD patterns of CaF₂:1% Yb³⁺, CaF₂:0.5% Pb²⁺ and CaF₂:1% Yb³⁺, 0.5% Pb²⁺ samples are shown in Fig. 1. The narrow and intense diffraction peaks indicate the well crystallization of the samples. The diffraction peaks of all the samples are consistent with the standard card (PDF #35-0816), suggesting that these materials have a cubic crystal structure.

We have measured the absorption spectra of CaF₂, CaF₂:0.5% Pb²⁺, CaF₂:1% Yb³⁺, and CaF₂:1% Yb³⁺, 0.5% Pb²⁺ powder samples in a wide spectral range from 200 to 1200 nm (Fig. 2). The spectra reveal the existence of Yb³⁺ ion (in NIR domain). The Yb³⁺ ions are characterized by a very broad band in the NIR spectral domain, corresponding to the ²F_{7/2}–²F_{5/2} transition (f–f transition). The ground state ²F_{7/2} split into three or four components and the excited state ²F_{5/2} split into two or three sublevels depending on the crystal field symmetry. The strongest absorption band peak appears at 979 nm.^{31,32} Fig. 2 shows the strong “absorption” in UV region (<400 nm) should be attributed to the Mie scattering. The absorption in NIR

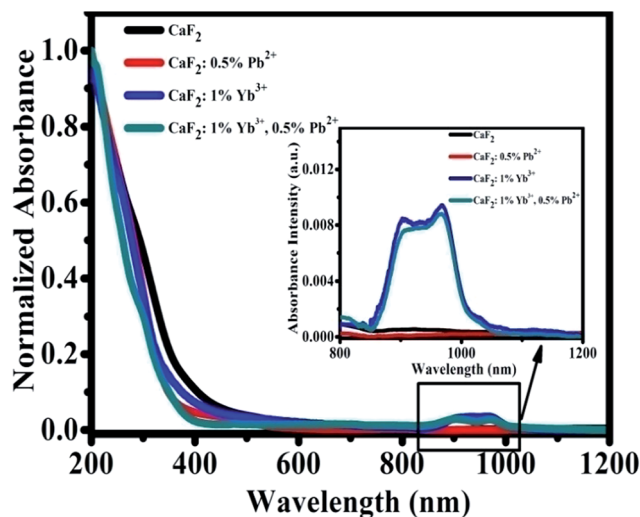


Fig. 2 Optical absorption spectra of CaF₂, CaF₂:0.5% Pb²⁺, CaF₂:1% Yb³⁺, and CaF₂:1% Yb³⁺, 0.5% Pb²⁺ samples.

region show that the samples with 1% Yb³⁺ dopant have significant absorption, and the sample of CaF₂:0.5% Pb²⁺ has not. Pb²⁺ ions cannot absorb NIR light directly therefore cannot influence the NIR absorption spectra of Yb³⁺ ions.

Under the excitation of a 978 nm laser, the CaF₂:Yb³⁺ polycrystalline powders showed 343 nm and 500 nm UC emission spectra, which has been previously reported.²⁸ Our previous works has demonstrated that the 343 nm UC fluorescence is the TCL of Yb³⁺-trimers, as shown in Fig. 3(a). With the increase of doped Yb³⁺ concentration, the UV emission peaked at 343 nm first increases and then decreases, Fig. 3(b). The maximum UC emission intensity of Yb³⁺-trimers is obtained at the concentration of Yb³⁺ reaches 1 mol%. Spectral analysis indicated that the 500 nm UC emission came from Yb³⁺-dimers in the CaF₂:Yb³⁺ polycrystalline, as shown in Fig. 3(c). With the increase of doped Yb³⁺ concentration, the maximum UC emission intensity of Yb³⁺-dimers is obtained at the concentration of Yb³⁺ reaches 1 mol%, Fig. 3(d).

Under 978 nm excitation, the UV emission spectra of CaF₂:x% Yb³⁺, y% Pb²⁺ (x = 0, 1; y = 0, 0.3, 0.5, 1, 2, 3, 4) were recorded at room temperature, as shown in Fig. 4(a). No luminescence can be found in the sample of CaF₂:0.5% Pb²⁺ throughout the entire spectral region because the NIR excitation cannot be absorbed by Pb²⁺ ions.³³ On the other hand, an obvious UV fluorescence peaked at 343 nm can be seen in the spectrum of CaF₂:1% Yb³⁺. Our previous works has demonstrated that the 343 nm upconversion fluorescence is the TCL of Yb³⁺-trimers.²⁸ After doping small amounts of Pb²⁺ ions (e.g. 0.3%) in CaF₂:1% Yb³⁺, the TCL intensity became lower and a new UV luminescence appeared at 383 nm. Fig. 4(a) show the cooperative upconversion spectra against Pb²⁺ concentrations. It is quite clear that the TCL (343 nm) peak follow a similar trend, that is, a gradual decrease in the emission intensities until they disappear when Pb²⁺ concentration reaches 4 mol%. With the increase of doped Pb²⁺ concentration, the UV emission peaked at 383 nm first increases and then decreases. It reaches

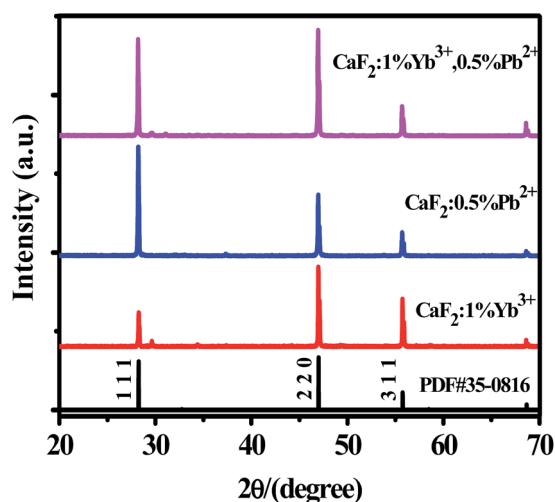


Fig. 1 XRD patterns of CaF₂:x% Yb³⁺, y% Pb²⁺.



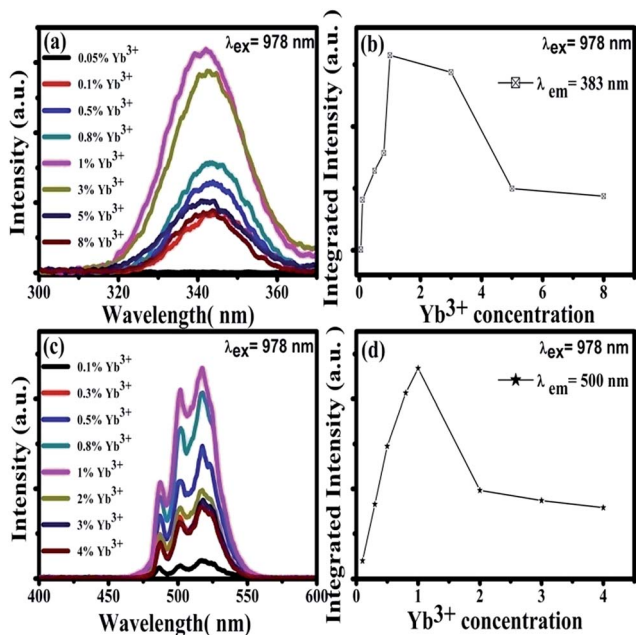


Fig. 3 (a) Emission spectra (300–400 nm) of $\text{CaF}_2:x\% \text{Yb}^{3+}$ ($x = 0.05, 0.1, 0.5, 0.8, 1, 3, 5, 8$) upon 978 nm excitation at room temperature. (b) Integrated intensity dependence of 343 nm UC emissions on the doping concentration of Yb^{3+} . (c) Emission spectra (400–600 nm) of $\text{CaF}_2:x\% \text{Yb}^{3+}$ ($x = 0.1, 0.3, 0.5, 0.8, 1, 2, 3, 4$) upon 978 nm excitation at room temperature. (d) Integrated intensity dependence of 500 nm UC emissions on the doping concentration of Yb^{3+} .

the maximum at 0.5 mol% doping concentration of Pb^{2+} ions and disappears at 4 mol% Pb^{2+} ions. Therefore, it is reasonable for us to deduce that the emission peaked at 383 nm comes from the excited Pb^{2+} ions, and further investigation (show later) exhibits that it comes from the $^3\text{P}_0 \rightarrow ^1\text{A}_{1g}$ transition of Pb^{2+} ions. Now, the problem is, in this system, what induces the Pb^{2+} ions excited under the NIR irradiation? In ref. 28, we reported the UV UCL from Gd^{3+} ions upon 978 nm excitation and verified that the excitation of Gd^{3+} ions came from the cooperative energy transfer of four excited Yb^{3+} ions (Yb^{3+} -tetramer). In the case of Pb^{2+} ions, the same mechanism is also existence; namely, the excitation of Pb^{2+} ions may originate from the cooperative sensitization of Yb^{3+} -trimers or Yb^{3+} -tetramers.

We have already shown that the cooperative transition probability of an Yb^{3+} -trimer is much higher than that of an Yb^{3+} -tetramer,³⁰ indicating that it has a larger possibility for excited Yb^{3+} -trimers to transfer their energy to the Pb^{2+} ions than that for excited Yb^{3+} -tetramers. Moreover, it can be seen from Fig. 4(a) that the increase of Pb^{2+} concentration induces not only the fluorescence of Pb^{2+} ions but also the decrease of TCL from Yb^{3+} -trimers. Combining the above experimental phenomena with the fact that Pb^{2+} ions cannot absorb 978 nm excitation light directly, it is not difficult to deduce that the excitation of Pb^{2+} ions originates from the cooperative sensitization of more than two excited Yb^{3+} ions, in other words, from the cooperative energy transfer of Yb^{3+} -trimers. It can be seen from Fig. 4(a) that the increment of Pb^{2+} luminescence is much smaller than the decrement of TCL, indicating that not all

excitation energy of Yb^{3+} -trimers lost in the energy transfer to Pb^{2+} ions. The UV emissions of 343 nm and 383 nm completely disappear when the doping concentration of Pb^{2+} ions reaches 4%, which strongly suggests that doped Pb^{2+} ions lead to the occurrence of cooperative energy transfer from Yb^{3+} -trimers. According to above analysis, we propose here that the excitation of Pb^{2+} ions comes from the energy transfer from excited Yb^{3+} -trimers.

Furthermore, we studied the influence of Pb^{2+} concentration to the cooperative luminescence from Yb^{3+} -dimers (DCL). As shown in Fig. 4(b), the intensity of green DCL from Yb^{3+} -dimers becomes lower when the concentration of Pb^{2+} ions increases gradually. The DCL emission band in the green spectral region has unique spectral structure even at room temperature. When the doping concentration of Pb^{2+} ions increases gradually from 0% to 6% in $\text{CaF}_2:1\% \text{Yb}^{3+}$ samples, the DCL decreases and until completely disappears at 6% Pb^{2+} doping concentration. The transition probabilities of DCL and TCL in CaF_2 are calculated to be $2.6 \times 10^{-2} \text{ s}^{-1}$ and $1.8 \times 10^{-6} \text{ s}^{-1}$, respectively.³⁰ Although the TCL from Yb^{3+} -trimers disappears when the doped concentration of Pb^{2+} ions is 4%, the DCL from Yb^{3+} -dimers exists until the doping concentration of Pb^{2+} ions reaches 6%. Fig. 4(c) shows the temperature-dependent UC emission spectra of $\text{CaF}_2:1\% \text{Yb}^{3+}, 0.5\% \text{Pb}^{2+}$ during cooling under the excitation of a 978 nm laser. As the temperature decreases, the peak positions of all emission bands (343 and 383 nm) exhibit no significant changes, whereas the UC emission intensities increase monotonously. It is well known that the

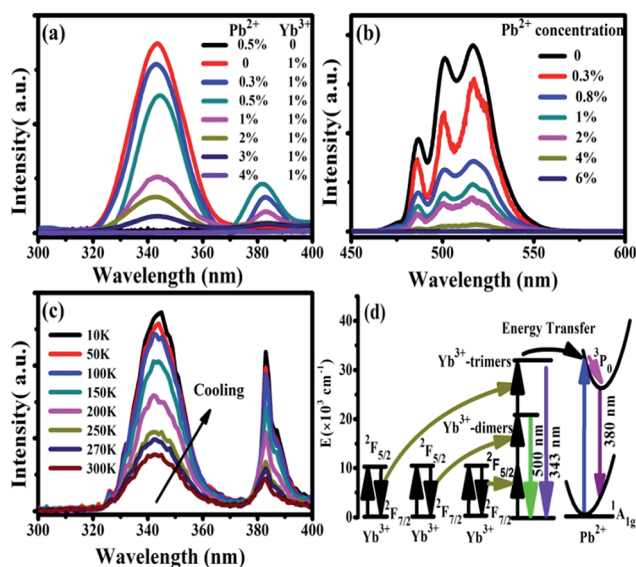


Fig. 4 (a) Emission spectra (300–400 nm) of $\text{CaF}_2:x\% \text{Yb}^{3+}, y\% \text{Pb}^{2+}$ ($x = 0, 1; y = 0, 0.3, 0.5, 1, 2, 3, 4$) upon 978 nm excitation at room temperature (b) emission spectra (450–600 nm) of $\text{CaF}_2:1\% \text{Yb}^{3+}, y\% \text{Pb}^{2+}$ ($y = 0, 0.3, 0.8, 1, 2, 4, 6$) upon 978 nm excitation at room temperature (c) temperature dependent UC emission spectra of $\text{CaF}_2:1\% \text{Yb}^{3+}, 0.5\% \text{Pb}^{2+}$ during cooling (d) schematic energy level diagram of Yb^{3+} and Pb^{2+} . The cooperative energy transfer from three excited Yb^{3+} ions to one Pb^{2+} ion is exhibited by using black arrows. The magenta arrow indicates the non-radiative relaxation process in Pb^{2+} ions.



luminescence efficiencies are strongly temperature dependent, and usually the higher temperature would result in lower luminescence efficiency due to the strong nonradiative loss as the temperature rises. Fig. 4(d) shows a schematic of energy diagram for the cooperative energy transfer of three Yb^{3+} ions. In the schematic diagram, Pb^{2+} ions are excited by the sensitization of Yb^{3+} -trimers, and then relax to the bottom of the excited state through a non-radiative way. When the excited Pb^{2+} ions make a transition from the excited state $^3\text{P}_0$ to the ground state $^1\text{A}_{1g}$, the UC emission at 383 nm can be observed. The cooperative UC process includes four ions, one Pb^{2+} ion and three Yb^{3+} ions. Under the excitation of 978 nm NIR, the multi-ion system emits an UV photon of 383 nm. The $^3\text{P}_0 \rightarrow ^1\text{A}_{1g}$ transition of Pb^{2+} ions is forbidden since $\Delta S = 1$ and $\Delta J = 0$. However, selection rules are not absolute, especially for heavy ions (such as Pb^{2+}). In a heavy ion, the coupling of spin-orbit is strong, which mixes spin triplet ($S = 1$) and singlet ($S = 0$) and lifts the spin forbidden partly. As a result, the spin forbidden transitions in some heavy ions can be observed. It can be seen from Fig. 4(d) that the purple line shows the radiative transition of Pb^{2+} ions. Fig. 5 shows the intensity dependence of 343 nm, 383 nm, and 500 nm UC emissions on the doping concentration of Pb^{2+} . While the concentration of Yb^{3+} keeps at 1%, the best concentration of Pb^{2+} ions is 0.5% for the emission of Pb^{2+} ions at 383 nm.

The UV excitation spectrum of 383 nm emission from $\text{CaF}_2:1\% \text{Yb}^{3+}, 0.5\% \text{Pb}^{2+}$ is peaked at 330 nm (due to Pb^{2+} ions), as shown in Fig. 6(a). The excitation band is highly overlapped with the TCL band peaked at 343 nm, which satisfies the condition of cooperative sensitization from excited Yb^{3+} -trimers to Pb^{2+} ions and gives further the excitation mechanism of 383 nm UCL. The 383 nm luminescence of $\text{CaF}_2:0.5\% \text{Pb}^{2+}$ upon 330 nm excitation shows that this luminescence comes from Pb^{2+} ions, as shown in Fig. 6(b). Under 330 nm excitation, we also recorded the UV emission spectrum of $\text{CaF}_2:1\% \text{Yb}^{3+}, 0.5\% \text{Pb}^{2+}$ (red line). This spectral result is similar to that of the

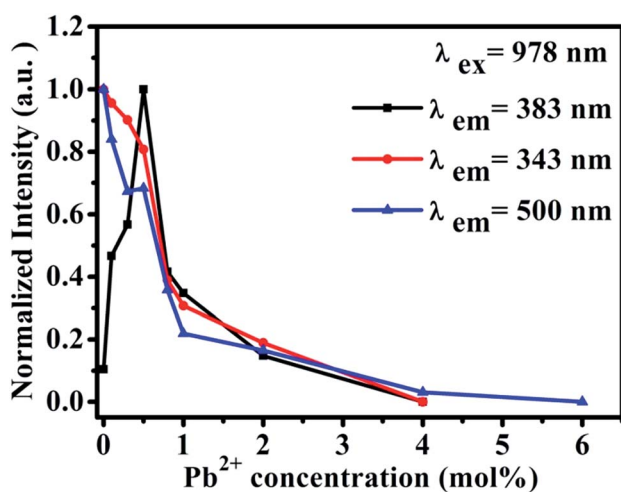


Fig. 5 Intensity dependence of 343 nm, 383 nm and 500 nm UC emissions on the doping concentration of Pb^{2+} in $\text{CaF}_2:1\% \text{Yb}^{3+}, x\% \text{Pb}^{2+}$ ($x = 0, 0.3, 0.5, 0.8, 1, 2, 3, 4, 6$).

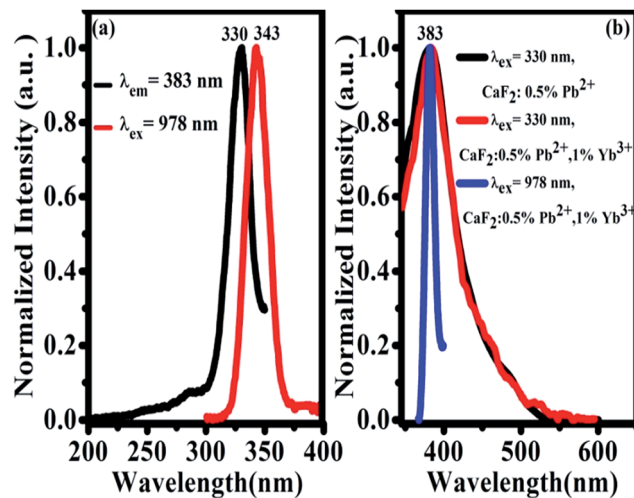


Fig. 6 (a) UC emission spectrum upon 978 nm excitation of Yb^{3+} -trimers (red line) and excitation spectrum for 383 nm Pb^{2+} emission in $\text{CaF}_2:1\% \text{Yb}^{3+}, 0.5\% \text{Pb}^{2+}$ (black line) at room temperature; (b) emission spectra of $\text{CaF}_2:0.5\% \text{Pb}^{2+}$ (black) and $\text{CaF}_2:1\% \text{Yb}^{3+}, 0.5\% \text{Pb}^{2+}$ (red) upon 330 nm excitation, and the UCL spectrum of $\text{CaF}_2:1\% \text{Yb}^{3+}, 0.5\% \text{Pb}^{2+}$ (blue) upon 978 nm excitation at room temperature, respectively.

sample without Yb^{3+} doping, indicating that the down-conversion emission of Pb^{2+} ions is not influenced by Yb^{3+} doping. The absorption bands of Pb^{2+} ions in CaF_2 are peaked at 246 nm, 306 nm, and a broad band between 310 nm and 450 nm.³³ On the other hand, upon 978 nm NIR excitation, a similar UV emission (Fig. 6(b), blue line) peaked at 383 nm was also observed in $\text{CaF}_2:1\% \text{Yb}^{3+}, 0.5\% \text{Pb}^{2+}$. Therefore, it is reasonable for us to attribute the UV emission peaked at 383 nm to the $^3\text{P}_0 \rightarrow ^1\text{A}_{1g}$ transition of Pb^{2+} ions. The widths of black and red peaks are almost the same and wider than that of the blue one. There are various activator symmetry sites for the codoped Pb^{2+} ions in the powder samples but only a special part of them can be excited by the ET from the excited Yb^{3+} -trimers, therefore the UCL band from Pb^{2+} ions is rather narrow.

In order to study the cooperative energy transfer from Yb^{3+} -trimers to Pb^{2+} ions, we studied the excited state dynamics of $\text{CaF}_2:1\% \text{Yb}^{3+}, 0.5\% \text{Pb}^{2+}$ under the excitation of 978 nm. At 10 K and 300 K, we recorded the decay curve of TCL from $\text{CaF}_2:1\% \text{Yb}^{3+}, 0.5\% \text{Pb}^{2+}$ under the chopped 978 nm excitation by using an oscilloscope. The energy transfer processes are often dependent on temperature. It can be seen from Fig. 7(a) that these decay curves have no rising edge, which indicates that TCL (~ 343 nm) come from the direct excitation of 978 nm and no energy transfer process exists. The lifetime of Yb^{3+} -trimers a little decrease from 0.487 ms to 0.423 ms. In addition, the higher the temperature the shorter the life time due to dependence of nonradiative multiphonon relaxation processes on temperature. However, the 383 nm UCL of Pb^{2+} ions shows a rising edge, as shown in Fig. 7(b), which means that the excitation of Pb^{2+} comes from energy transfer. The lifetime of Pb^{2+} excited state is long (0.475 ms) due to the $^3\text{P}_0 \rightarrow ^1\text{A}_{1g}$ transition is strongly forbidden. As can be seen in Fig. 7(c), the lifetime of TCL gradually decreases with the increase of Pb^{2+}



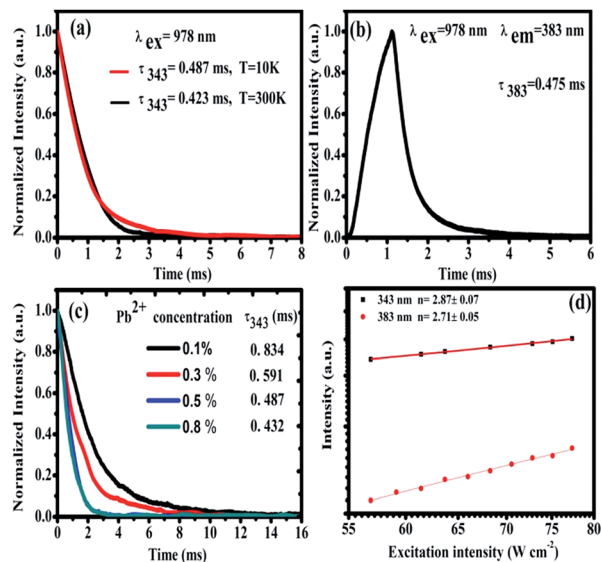


Fig. 7 (a) Temperature dependent fluorescence decay curves of 343 nm TCLs. (b) Fluorescence decay curve of the UCL at 383 nm from Pb^{2+} ions upon 978 nm excitation at 10 K. (c) Fluorescence decay curves of 343 nm TCL from Yb^{3+} -trimers with different Pb^{2+} concentrations under 978 nm excitation in $\text{CaF}_2:1\% \text{Yb}^{3+}, x\% \text{Pb}^{2+}$ ($x = 0.1\%, 0.3\%, 0.5\%$, and 0.8%) at 10 K, respectively. (d) Double-logarithmic plots of the pump-power dependent UC emission intensity recorded under 978 nm excitation.

doping concentration, which indicates the cooperative energy transfer from Yb^{3+} -trimers to Pb^{2+} ions. Fig. 7(d) shows the typical double-logarithmic plots of luminescence intensity I_f versus the pump power density I_{NIR} . The n value can be obtained from the slope of the linear fit. The fitting results of square and circle are approximately 2.87 ± 0.07 and 2.71 ± 0.05 for 343 and 383 nm emissions, respectively. These n values reveal that both the emissions at 343 and 383 nm belong to three-photon UC processes.

Conclusions

In summary, we synthesized $\text{CaF}_2:\text{Pb}^{2+}, \text{Yb}^{3+}$ phosphors through a coprecipitation method. Under the excitation of 978 nm, not only the TCL at 343 nm from Yb^{3+} -trimers was observed but also the UV UCL at 383 nm from Pb^{2+} ions was recorded for the first time. Experimental results shows that the population of Pb^{2+} excited states originates from the cooperative energy transfer from excited Yb^{3+} -trimers. With the increase of Pb^{2+} concentration, both of the TCL and the UV UCL from Pb^{2+} ions decrease and disappear.

Experimental section

Powder samples of CaF_2 doped with Yb^{3+} (0, 1 mol%) and Pb^{2+} (0, 0.3, 0.5, 0.8, 1, 2, 3, 4 mol%) were prepared by a conventional co-precipitation method by using $\text{Ca}(\text{NO}_3)_2 \cdot 4\text{H}_2\text{O}$ (99%, Aladdin), $\text{Yb}(\text{NO}_3)_3 \cdot 5\text{H}_2\text{O}$ (99.99%, Aladdin), $\text{Pb}(\text{NO}_3)_2$ (99.999%, Aladdin), and NH_4HF_2 (99.99%, Aladdin) as the raw materials. Firstly, standard aqueous solutions of 0.5 mol l^{-1}

$\text{Yb}(\text{NO}_3)_3 \cdot 5\text{H}_2\text{O}$, $0.01 \text{ mol l}^{-1} \text{ Pb}(\text{NO}_3)_2$, and $0.5 \text{ mol l}^{-1} \text{ Ca}(\text{NO}_3)_2 \cdot 4\text{H}_2\text{O}$ were prepared. A stoichiometric amounts of $\text{Yb}(\text{NO}_3)_3 \cdot 5\text{H}_2\text{O}$, $\text{Pb}(\text{NO}_3)_2$, and $\text{Ca}(\text{NO}_3)_2 \cdot 4\text{H}_2\text{O}$ aqueous solutions were put in a beaker with 30 min constant stirring, and then the mixture was added dropwise to NH_4HF_2 aqueous solution under constant stirring for 1 h to get uniform precipitations. The obtained precipitations were then washed several times with distilled water to remove the remained NO_3^- and F^- ions. The products were dried at 95°C for 12 h and then calcined at 1200°C for 2 h in air. All the samples were synthesized under the identical conditions. The luminescence spectra were recorded with a one-meter monochromator (SPEX 1000M; HORIBA Jobin Yvon Inc., Edison, NJ, USA) equipped with an 1800 lines per mm grating. The excitation light source was a power-adjustable continuous wave laser diode (978 nm, 10 W; BWT Beijing Ltd, Beijing, China). The mean power of this excitation light source is 10 W, and the NIR laser was focused on the sample by a lens. A digital oscilloscope (DPO4104B, bandwidth 1 GHz, sampling rate 5 GS s^{-1} ; Tektronix, Shanghai, China), a power-adjustable continuous wave laser diode (CW 978 nm, 10 W), and a chopper were used to record decay curves.

Acknowledgements

This work supported by the National Natural Science Foundation of China (NSFC) (11274139, 11474132) and the Natural Science Foundation of Xinjiang Province, China (2015211C295).

Notes and references

- 1 A. J. Silversmith, W. Lenth and R. M. Macfarlane, Green infrared-pumped erbium upconversion laser, *Appl. Phys. Lett.*, 1987, **51**, 1977.
- 2 R. M. Macfarlane, F. Tong, A. J. Silversmith and W. Lenth, Violet cw neodymium upconversion laser, *Appl. Phys. Lett.*, 1988, **52**, 1300.
- 3 T. Danger, J. Koetke, R. Brede, E. Heumann, G. Huber and B. H. T. Chai, Spectroscopy and green upconversion laser emission of Er^{3+} -doped crystals at room temperature, *J. Appl. Phys.*, 1994, **76**, 1413.
- 4 L. F. Johnson and H. J. Guggenheim, Laser emission at 3μ from Dy^{3+} in BaY_2F_8 , *Appl. Phys. Lett.*, 1973, **23**, 96.
- 5 M. F. Joubert, Photon avalanche upconversion in rare earth laser materials, *Opt. Mater.*, 1999, **11**, 181.
- 6 J. F. Suyver, A. Aebischer, D. Biner, P. Gerner, J. Grimm, S. Heer, K. W. Kramer, C. Reinhard and H. U. Gudel, Novel materials doped with trivalent lanthanides and transition metal ions showing near-infrared to visible photon upconversion, *Opt. Mater.*, 2005, **27**, 1111.
- 7 M. Pollnau, D. R. Gamelin, S. R. Luthi and H. U. Gudel, Power dependence of upconversion luminescence in lanthanide and transition-metal-ion systems, *Phys. Rev. B: Condens. Matter Mater. Phys.*, 2000, **61**, 3337.
- 8 E. H. Song, S. Ding, M. Wu, S. Ye, F. Xiao, S. F. Zhou and Q. Y. Zhang, Anomalous NIR Luminescence in Mn^{2+} -Doped Fluoride Perovskite Nanocrystals, *Adv. Opt. Mater.*, 2014, **2**, 670.



- 9 L. L. Wang, X. J. Xue, F. Shi, D. Zhao, D. S. Zhang, K. Z. Zheng, G. F. Wang, C. F. He, R. Kim and W. P. Qin, Ultraviolet and violet upconversion fluorescence of europium(III) doped in YF_3 nanocrystals, *Opt. Lett.*, 2009, **34**, 2781.
- 10 E. H. Song, S. Ding, M. Wu, S. Ye, F. Xiao, G. P. Dong and Q. Y. Zhang, Temperature-tunable upconversion luminescence of perovskite nanocrystals $\text{KZnF}_3:\text{Yb}^{3+}, \text{Mn}^{2+}$, *J. Mater. Chem. C*, 2013, **1**, 4209.
- 11 N. Rakov, R. B. Guimaraes and G. S. Maciel, Photon up-conversion production in Tb^{3+} - Yb^{3+} co-doped CaF_2 phosphors prepared by combustion synthesis, *Mater. Res. Bull.*, 2016, **74**, 103.
- 12 F. F. Huang, X. Q. Liu, Y. Y. Ma, S. Kang, L. L. Hu and D. P. Chen, Origin of near to middle infrared luminescence and energy transfer process of $\text{Er}^{3+}/\text{Yb}^{3+}$ co-doped fluorotellurite glasses under different excitations, *Sci. Rep.*, 2015, **5**, 8233.
- 13 W. Strek, B. Cichy, L. Radosinski, P. Gluchowski, L. Marciniak, M. Lukaszewicz and D. Hreniak, Laser-induced white-light emission from graphene ceramics-opening a band gap in graphene, *Light: Sci. Appl.*, 2015, **4**, e237.
- 14 W. P. Qin, D. S. Zhang, D. Zhao, L. L. Wang and K. Z. Zheng, Near-infrared photocatalysis based on $\text{YF}_3:\text{Yb}^{3+} \text{ Tm}^{3+}/\text{TiO}_2$ core/shell nanoparticles, *Chem. Commun.*, 2010, **46**, 2304.
- 15 X. Y. Guo, W. H. Di, C. F. Chen, C. X. Liu, X. Wang and W. P. Qin, Enhanced near-infrared photocatalysis of $\text{NaYF}_4:\text{Yb}$, $\text{Tm}/\text{CdS}/\text{TiO}_2$ composites, *Dalton Trans.*, 2014, **43**, 1048.
- 16 F. Auzel, Upconversion and anti-stokes processes with f and d ions in solids, *Chem. Rev.*, 2004, **104**, 139.
- 17 C. P. Joshi and S. V. Moharil, Luminescence of Pb^{2+} in some aluminates prepared by combustion synthesis, *Phys. Status Solidi B*, 2000, **220**, 985.
- 18 H. F. Folkerts, J. Zuidema and G. Blasse, The luminescence of Pb^{2+} in lead compounds with one-dimensional chains, *Solid State Commun.*, 1996, **99**, 655.
- 19 H. F. Folkerts and G. Blasse, Two types of luminescence from Pb^{2+} in alkaline-earth carbonates with the aragonite structure, *J. Phys. Chem. Solids*, 1996, **57**, 303.
- 20 D. F. Anderson, J. A. Kierstead, P. Lecoq, S. Stollb and C. L. Woody, A search for scintillation in doped and orthorhombic lead fluoride, *Nucl. Instrum. Methods Phys. Res., Sect. A*, 1994, **342**, 473.
- 21 S. A. Kazanskii, A. I. Ryskin, A. E. Nikiforov, A. Y. Zaharov, M. Y. Ougrumov and G. S. Shakurov, EPR spectra and crystal field of hexamer rare-earth clusters in fluorites, *Phys. Rev. B: Condens. Matter Mater. Phys.*, 2005, **72**, 014127.
- 22 V. A. Chernyshev, A. E. Nikiforov and A. D. Nazemnikh, Hexamer clusters in $\text{MeF}_2:\text{Yb}^{3+}$ ($\text{Me} = \text{Ca}, \text{Sr}, \text{Ba}$), *J. Phys.: Conf. Ser.*, 2011, **324**, 012025.
- 23 E. Nakazawa, Cooperative Luminescence in YbPO_4 , *Phys. Rev. Lett.*, 1970, **25**, 1710.
- 24 F. Varsanyi and G. H. Dieke, Ion-pair resonance mechanism of energy transfer in rare earth crystal fluorescence, *Phys. Rev. Lett.*, 1961, **7**, 442.
- 25 J. Wang, R. R. Deng, M. A. MacDonald, B. L. Chen, J. K. Yuan, F. Wang, D. Z. Chi, T. S. A. Hor, P. Zhang, G. K. Liu, Y. Han and X. Liu, Enhancing multiphoton upconversion through energy clustering at sublattice level, *Nat. Mater.*, 2014, **13**, 157.
- 26 X. T. Wei, J. B. Zhao, W. P. Zhang, Y. Li and M. Yin, Cooperative energy transfer in Eu^{3+} , Yb^{3+} codoped Y_2O_3 phosphor, *J. Rare Earths*, 2010, **28**, 166.
- 27 J. L. He, Z. G. Zhou, H. Zhan and A. X. Lin, Intense red fluorescence from Ho/Yb codoped tellurite glasses, *J. Non-Cryst. Solids*, 2014, **383**, 157.
- 28 W. P. Qin, Z. Y. Liu, C. N. Sin, C. F. Wu, G. S. Qin, Z. Chen and K. Z. Zheng, Multi-ion cooperative processes in Yb^{3+} clusters, *Light: Sci. Appl.*, 2014, **3**, e193.
- 29 T. Aidilibike, Y. Y. Li, J. J. Guo, X. H. Liu and W. P. Qin, Blue upconversion emission of Cu^{2+} ions sensitized by Yb^{3+} -trimers in CaF_2 , *J. Mater. Chem. C*, 2016, **4**, 2123.
- 30 W. P. Qin, S. Cholnam, Z. Y. Liu, G. S. Qin and C. F. Wu, Theory on cooperative quantum transitions of three identical lanthanide ions, *J. Opt. Soc. Am. B*, 2015, **32**, 303.
- 31 W. Low, Paramagnetic and Optical Spectra of Ytterbium in the Cubic Field of Calcium Fluoride, *Phys. Rev.*, 1960, **118**, 1608.
- 32 V. Petit, P. Camy, J. L. Doualan, X. Portier and R. Moncorge, Spectroscopy of $\text{Yb}^{3+}:\text{CaF}_2$: From isolated centers to clusters, *Phys. Rev. B: Condens. Matter Mater. Phys.*, 2008, **78**, 085131.
- 33 I. Nicoara, M. Munteanu, N. Pecingina-Garjoaba, M. Stef, E. Preda and A. Lucaci, Dielectric spectra of doped and X-ray irradiated calcium fluoride crystals, *Phys. Status Solidi C*, 2007, **4**, 1234.

